ANL-5711
Reactors-Power

ARGONNE NATIONAL LABORATORY
P. O. Box 299
Lemont, Illinois

EBWR PHYSICS EXPERIMENTS

by

J. A. Thie

Experiments performed by:

N. Balai	A. S. Jameson
R. E. Bailey	W. C. Lipinski
J. A. Beidelman	R. A. Mattson
S. A. Bernsen	F. H. Martens
C. F. Bullinger	C. V. Pearson
J. A. DeShong	C. K. Soppet
L. W. Fromm	J. A. Thie
R. J. Gariboldi	J. M. West (Chief Project Engineer)
V. C. Hall	
J. M. Harrer	E. A. Wimunc
A. H. Heineman	H. R. Zeitlin
R. C. Howard	C. B. Zitek*

July 1957

*Loaned Employee from Commonwealth Edison Co.

Operated by The University of Chicago
under
Contract W-31-109-eng-38

DISCLAIMER

TABLE OF CONTENTS

	Page
ABSTRACT	5
I. INTRODUCTION	5
II. PRE-POWER GENERATION EXPERIMENTS	6
A. Approach to Criticality	7
B. Reactivity Addition	9
C. Void Coefficient Measurement	10
D. Measurement of Worth of Boric Acid	12
E. Loading for Pressurized Power	13
F. Temperature Coefficient Measurements	16
III. POWER GENERATION EXPERIMENTS	18
A. Low-Pressure Power Operation	18
B. Boric Acid in the Pressurized Reactor	20
C. High-Power Operation	22
APPENDIX: Theoretical Basis of Reactor and Control Rod Reactivities	28

LIST OF FIGURES

Number	Title	Page
1	Approach to Criticality	7
2	Loading #19	8
3	Loading #26	9
4	Loading #33	9
5	Radial Variation of Void Coefficient - Core Loading No. 26 Control Rods in Upper 66% of Core	11
6	Temperature Void Addition to Core Loading No. 33	11
7	Boiling Void Removal From Core Loading No. 33	11
8	Loading #46	13
9	Axial Flux Distribution Two or More Inches from a Control Rod in Loading #46 at Room Temperature	14
10	Radial Flux and Power Distribution in Enriched Elements of Loading #46	14
11	Differential Worth of All 9 Control Rods as A Bank at Room Temperature in Loading #46	15
12	Integrated Temperature Coefficient for Loading #46 (unpoisoned)	17
13	Effect of Temperature on Differential Rod Worth	17
14	Power Oscillations at Low Pressure	20
15	Position of Control Rod Bank vs Temperature for Loading #46 (unpoisoned)	21
16	Reactivity in Boric Acid Addition to Loading #46	21
17	Boric Acid Removal from EBWR During 20-mw Operation	23
18	Ion Chamber Record at 20-mw Operation	23
19	Reactivity in Voids at 620 psig	25
20	Effect of H_3BO_3 on Reactivity in Voids	25
21	Reactivity in Voids as Influenced by Power, Rod Position and Boric Acid	26
22	Integral Rod Worth for Loading #46 at 68F	31
23	Effective Savings of Rodded Region as a Function of Rod Bank Position	31

LIST OF TABLES

Number	Title	Page
I	Fuel Element Structure	6
II	Reactivity and Void Coefficient of Loading #33	12
III	Boric Acid Worth in Loading #33	12
IV	Flux and Power Distribution at Room Temperature in Loading #46	15
V	Progression of Events in the First EBWR Nuclear Heating Experiment, December 18, 1956	19
VI	Reactivities of Loading #46	27
VII	Calculated Lattice Constants	29

EBWR PHYSICS EXPERIMENTS

by

J. A. Thie

ABSTRACT

The results of a number of zero power experiments, as well as the initial power generation experiments, are reported. These include critical mass determinations, control rod calibrations, void and temperature coefficient measurements, determinations of reactivity compensated by steam voids, and the effect of boric acid and control rods on power generation. A low-power, low-pressure, oscillation phenomenon, is described. Except for the latter, virtually all results are understood, quantitatively, by existing boiling reactor theories, although in some cases the desired precision is lacking.

I. INTRODUCTION

The Experimental Boiling Water Reactor (EBWR) is a light water-moderated and cooled, natural circulation, direct steam cycle, boiling reactor fueled with slightly enriched uranium. Reactor criticality was achieved on December 1, 1956. The following $2\frac{1}{2}$ weeks were confined to low-power experiments. Electricity (5 mw) at the rated power level (600 psi, 20 mw heat) was first generated on December 29, 1956.

Information about power plant experience will be reported elsewhere. The purpose of this report is to deal with phenomena associated directly with the reactor core.

The design concept for the EBWR provided for uninterrupted power dissipation: steam generated in the reactor is passed directly to the turbine for generation of electricity. The power generated is fed into the Laboratory distribution system. However, because of the power variations reflected by many of the experiments reported here, the steam output was dumped in its entirety to the condenser.

6

II. PRE-POWER GENERATION EXPERIMENTS

Since critical experiments involving slightly enriched uranium plates and light water have never been run, and also because the pressurized full-power loading was to be determined by open vessel experiments, a considerable effort was devoted to reactor physics experiments with unirradiated fuel. The phases in the program were:

(1) approach to criticality;
(2) addition of reactivity by expanding core size and trading elements;
(3) measuring void coefficients;
(4) measuring the worth of boric acid;
(5) adjustment of load to that needed for pressurized power; and
(6) measuring temperature coefficient.

Control rod calibrations were required in virtually all phases.

Four types of fuel assemblies are available (see Table I). Any given fuel assembly contains six identical plates in a box occupying a 48 in. (fuel height) x 4 in. x 4 in. cell. Thus various configurations of these fuel assemblies can be used to: (1) change the critical size of the core; (2) change the power distribution in the core; or (3) change the amount of reactivity corresponding to a given steam volume in the core.

Table I

FUEL ELEMENT STRUCTURE

Type	Thin Natural	Thick Natural	Thin Enriched	Thick Enriched
Symbol	T	H	ET	EH
Enrichment of U^{235}, %	0.72	0.72	1.44	1.44
Meat thickness, in.	0.174	0.239	0.174	0.239
Plate thickness, in.	0.214	0.279	0.214	0.279
Average water channel thickness, in.	0.453	0.388	0.453	0.388
$\left(\frac{H_2O\ Volume}{(U^{235} + U^{238})\ Volume}\right)$*	4.416	2.759	4.416	2.759
Nominal grams of U^{235} per 6-plate element	291.1	413.0	582.2	826.0
Average grams of U^{235} per 6-plate element found in loading #19	293.47	401.25	585.42	813.09

*Volume ratio is a reactor average and includes water in control rod channels.

7

A. Approach to Criticality

Nineteen subcritical loadings were made, ranging from loading #1 (3T + 3H + 3ET + 2EH) to loading #19 (14T + 14H + 25ET + 28EH). The procedure for each loading was:

(1) Slowly insert one element at a time into the water-filled core, observing counting rates and ion chamber currents; control rods are partially inserted.

(2) Take several counting rates at the completion of the loading with all control rods out.

(3) Move source and counter locations when necessary and obtain counting rates in the new position.

(4) Plot the reciprocal counting rate or current against the number of elements, and decide the next loading from this curve.

All loadings were designed to approximate a uniform mixture of the elements in the ratio: 18T:18H:38ET:38EH, mainly because many past calculations existed using this ratio.

Figure 1 shows the curve obtained for the last few loadings. The curvature existing when subcritical by many elements is in the expected direction because of the decrease in reactivity worth of one element as the reactor radius increases.

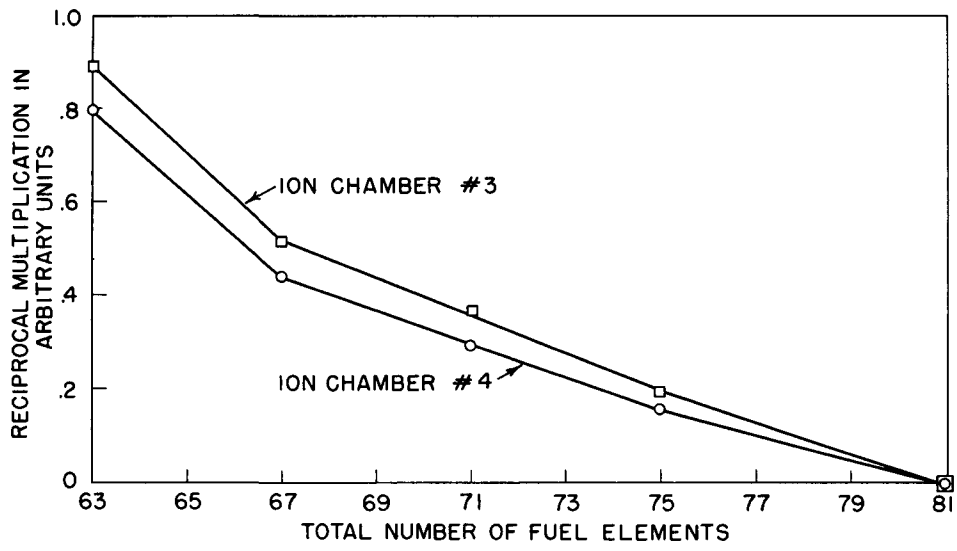

FIG. 1
APPROACH TO CRITICALITY

8

Figure 2 shows the last subcritical loading. With all control rods out the reactor approached its equilibrium multiplication with a time constant of approximately 270 sec, which indicated a reactivity of -0.03%, essentially a critical reactor.

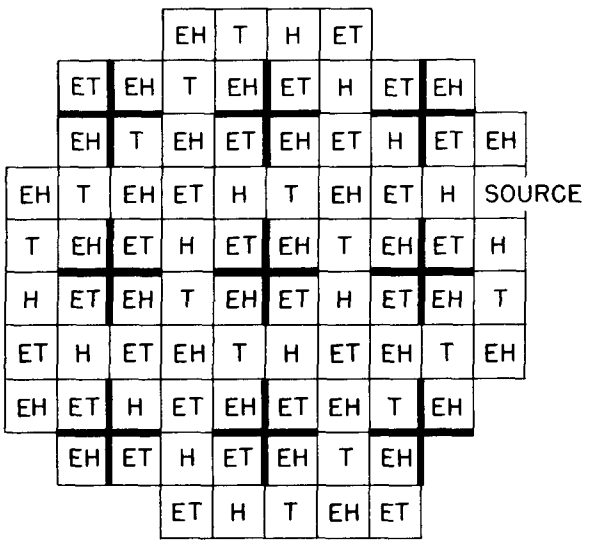

FIG. 2
LOADING #19

COMPOSITION: 28 THICK ENRICHED, EH
25 THIN ENRICHED, ET
14 THICK NATURAL, H
14 THIN NATURAL, T
81

kg OF U^{235}: 47.13

A comparison of the loading (14T + 14H + 25ET + 28EH) with that previously predicted to be critical by 2-group theory (6.83T + 6.83H + 14.43ET + 14.43EH) gives a measure of the error in the theory on a reactivity basis. The difference in the number of elements corresponds to 3.78%, while the difference in ratios of elements corresponds to -0.42%. Hence, 2-group theory overestimated the reactivity by 3.39%. Since this is within a previously estimated root mean square error of the theory (± 3.67%) based on cross-section errors, etc., the agreement between theory and experiment is satisfactory. (The criterion for choosing the enrichment and numbers of elements was that the theory could have been optimistic by twice its root mean square error, and still sufficient reactivity would have been available.) If the same 2-group methods used on EBWR are applied to a lattice[1] of 0.06-in. diameter, 1.143% enriched uranium rods with a water to uranium volume ratio of 4:1, the theory underestimates the reactivity by 1.33%.

---

[1] H. Kouts, et al., "Exponential Experiments with Slightly Enriched Uranium Rods in Ordinary Water." Proceedings of the International Conference on the Peaceful Uses of Atomic Energy held in Geneva 8 August - 20 August, 1955, Vol. 5, p. 183.

9

B. Reactivity Addition

Core Loading #26 (see Fig. 3) was built up in several steps from Loading #19. Measurement of the void coefficient indicated a negative value sufficient to permit a shift of the thin elements to the center. This is desirable from the standpoint of power generation, in which a low void coefficient (and, possibly, the absence of a thick-thin hot spot factor) may aid maximum power. The resultant loading (#33) is shown in Fig. 4.

All critical measurements and rod calibrations were done with all nine control rods level. This is the simplest configuration and also simplifies the calibration procedure.

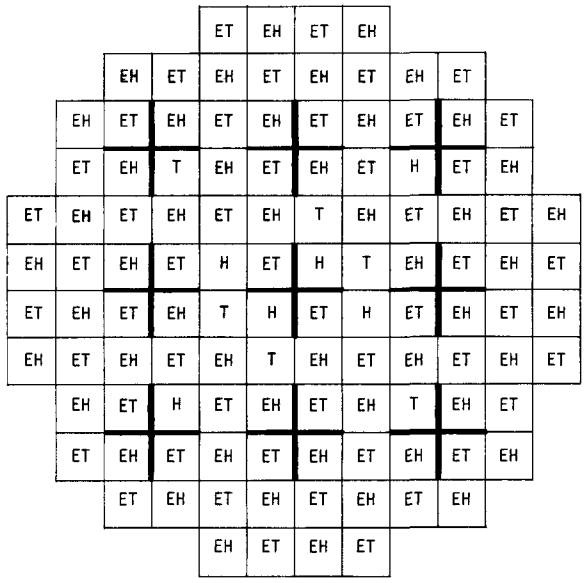

COMPOSITION: 50 THICK ENRICHED, EH
50 THIN ENRICHED, ET
6 THICK NATURAL, H
6 THIN NATURAL, T
112
kg OF U^{235}: 74.1

FIG. 3
LOADING #26

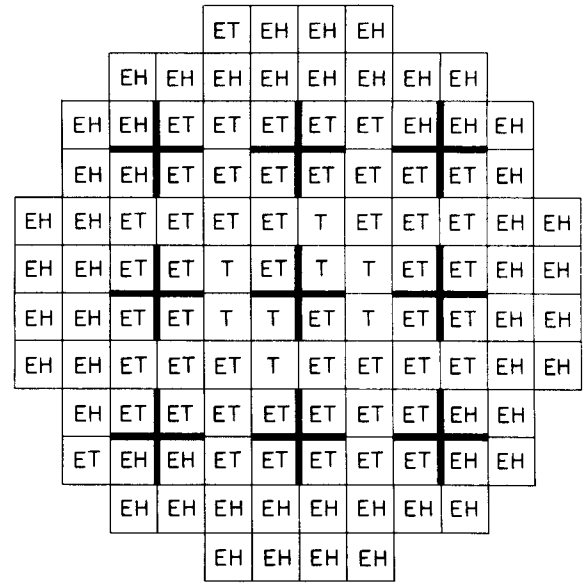

COMPOSITION: 54 THICK ENRICHED, EH
50 THIN ENRICHED, ET
8 THIN NATURAL, T
112
kg OF U^{235}: 75.5

FIG. 4
LOADING #33

C. Void Coefficient Measurement

Void coefficient measurements were performed by inserting perforated Styrofoam sheets[2] in the water channels of the fuel elements in core loadings #26 and #33. The Styrofoam sheets were designed to simulate the changes in moderator density (voids) associated with the temperature and boiling characteristics of the reactor.

The "temperature void" sheets with uniform perforations simulated a void volume proportional to the element's water density loss due to temperature. The "boiling void" sheets with nonuniform perforations simulated a void volume proportional to the element's nonuniform water density loss at full power.

The experiments were conducted in the following sequence of measurements:

(1) "temperature void" worth as a function of radial position in loading #26;

(2) "temperature void" coefficient of loading #33;

(3) "boiling void" coefficient of loading #33, with boric acid addition.

The results are plotted in Figs. 5 to 7. The abscissa in Figs. 6 and 7 is the average per cent of fuel assembly water channel volume occupied by the voids, exclusive of the voids in the control rod channels and in the reflector. Except for Fig. 5 the voids were uniformly distributed radially. All void coefficients determined are defined as:

$$\frac{d\rho}{dV} = \frac{\text{change in reactivity, in \%}}{100 \times (\text{change in water volume in channels}/\text{the original water volume})} .$$

As evidenced by Figs. 5 to 7, the values are sensitive to the control rod configuration. The fact that loading #33 is not significantly less negative than #26 (as would be expected) is not understood, although it may be due to its extra void content.

By adding boric acid to loading #33 and getting the control rods out, a more useful number is obtained (-0.067) for the removal of "boiling voids." A preliminary comparison using a crude 2-group, one-region approximation to this loading has the theory giving value of $d\rho/dV$ very near zero, and also erring on reactivity by 3.39%. However, using the modified theory of the

---

[2] J. A. DeShong, Jr. "Styrofoam Simulation of Boiling and Temperature Effects in the EBWR Cold Critical Experiments," ANL-5697 (March, 1957).

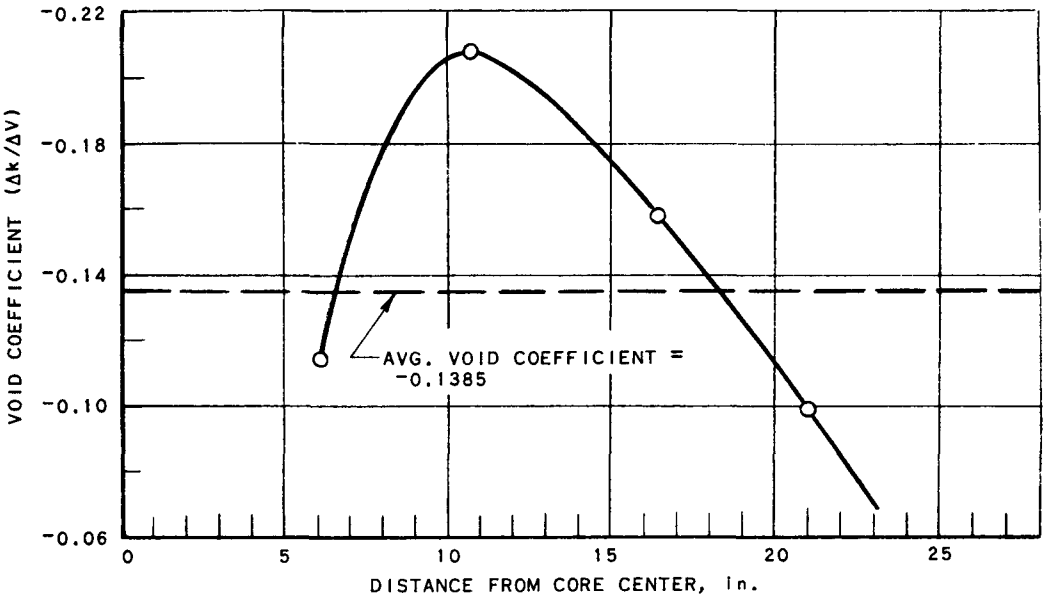

FIG. 5
RADIAL VARIATION OF VOID COEFFICIENT - CORE LOADING NO. 26 CONTROL RODS IN UPPER 66% OF CORE

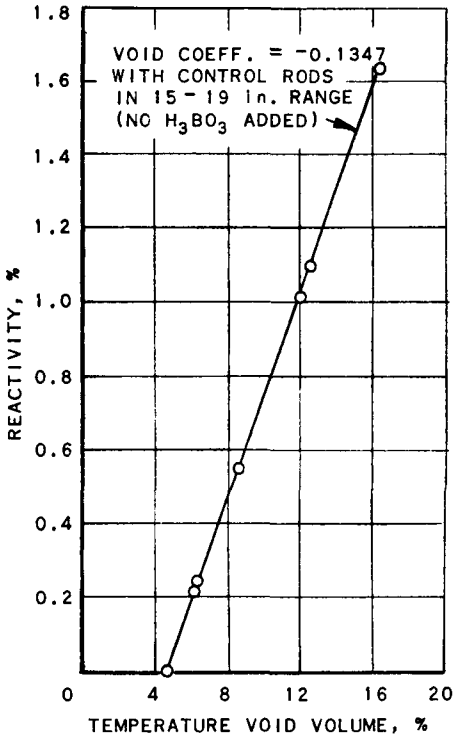

FIG. 6
TEMPERATURE VOID ADDITION TO CORE LOADING NO. 33

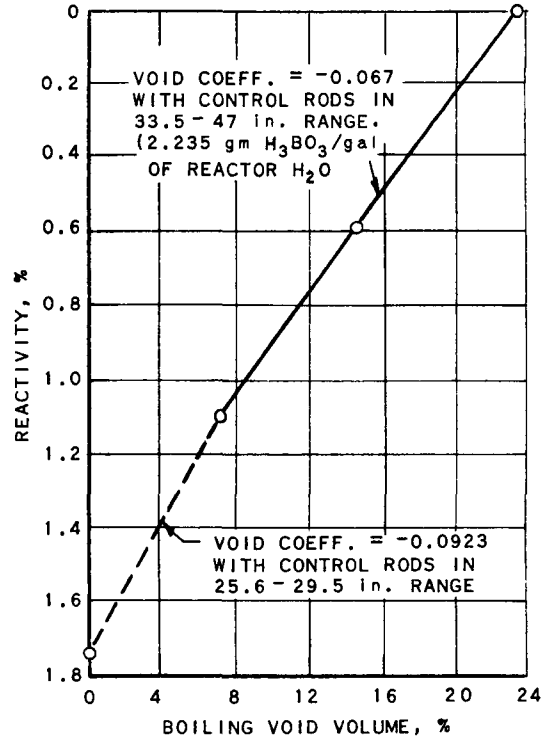

FIG. 7
BOILING VOID REMOVAL FROM CORE LOADING NO. 33

Appendix, in conjunction with perturbation theory (see Table VII), good agreement on reactivity and void coefficient is obtained:

Table II

REACTIVITY AND VOID COEFFICIENT OF LOADING #33

(With 2.235 gm of H_3BO_3 per gal and 23.75% Voids)

	Experimental	Theoretical
Reactivity, ρ	0	0.00382
Void Coefficient, $d\rho/dV$	- 0.067	- 0.0604

D. Measurement of Worth of Boric Acid

The use of boric acid serves the dual purpose of allowing the critical position of the rods to be varied in a given loading, as well as to obtain information on thermal utilization. To ensure thorough mixing, the acid was first dissolved in hot water, then poured into the reactor water, the latter being agitated by an air-bubble stream.

Again using a crude 2-group, one-region approximation to loading #33, Table III shows the good agreement with experiment, in this case, fortuitously good:

Table III

BORIC ACID WORTH IN LOADING #33

% voids in fuel plate water	% reactivity per gram of H_3BO_3 per gallon of H_2O	
	Experimental	Theoretical
0	-	1.780
23.75	1.417	1.427

E. Loading for Pressurized Power

A comparison of the borated and Styrofoam-loaded #33 with the xenon, samarium, and voids calculated to be present at 600 psi and equilibrium full power showed the need for additional reactivity. The final loading (#46) shown in Fig. 8 gave an additional 2.059% reactivity, which was more than adequate.

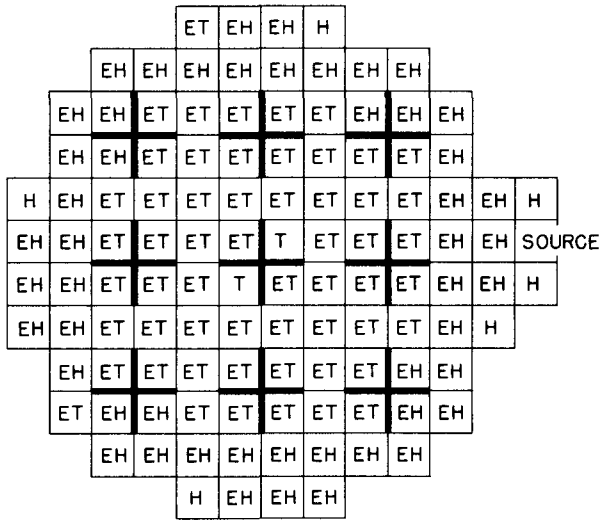

COMPOSITION: 50 THICK ENRICHED, EH
56 THIN ENRICHED, ET
6 THICK NATURAL, H
2 THIN NATURAL, T
114

kg OF U^{235}: 76.4

FIG. 8
LOADING #46

The logic behind the configuration of loading #46 is as follows:

Thin elements in the center give a less negative void coefficient and possibly more stable power. Natural elements in the center improve the radial maximum to average power density; whether this improves power stability is speculative. Defective thick enriched elements were replaced by thick naturals at the core edge. The choice of 114 elements is arbitrary, since presumably any number in the range from roughly 100 to 148 would give comparable power density performance.

Gold foils and wires were used to measure the flux distributions at room temperature in loading #46. The results are plotted in Figs. 9 and 10. The reflector savings of the upper control rod region on the lower fuel region inferred from the measured axial buckling in Table IV compares favorably with 20 cm obtained from the integral control rod worth (see Figs. 22 and 23 in the Appendix).

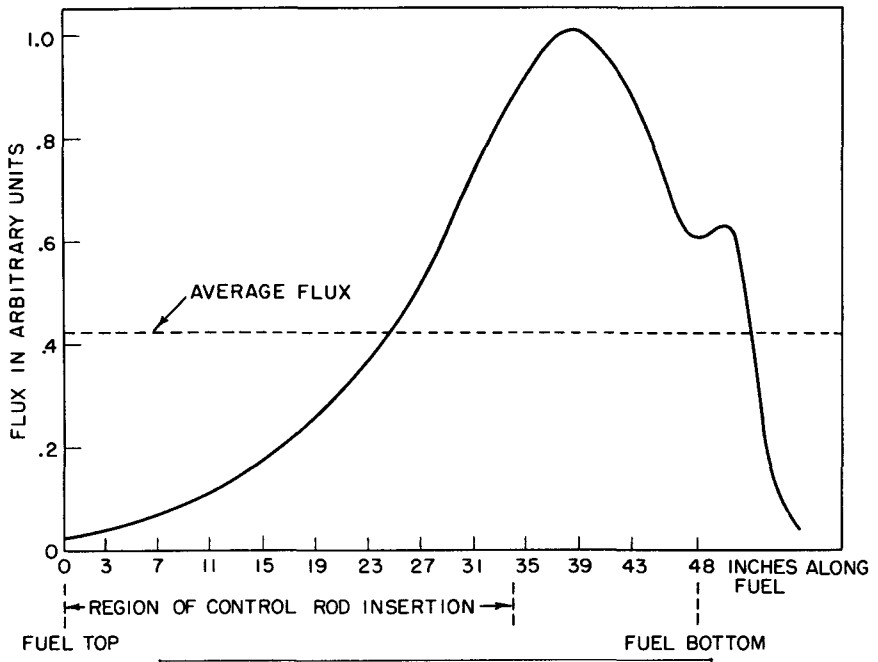

FIG. 9
AXIAL FLUX DISTRIBUTION TWO OR MORE INCHES FROM A CONTROL ROD IN LOADING #46 AT ROOM TEMPERATURE

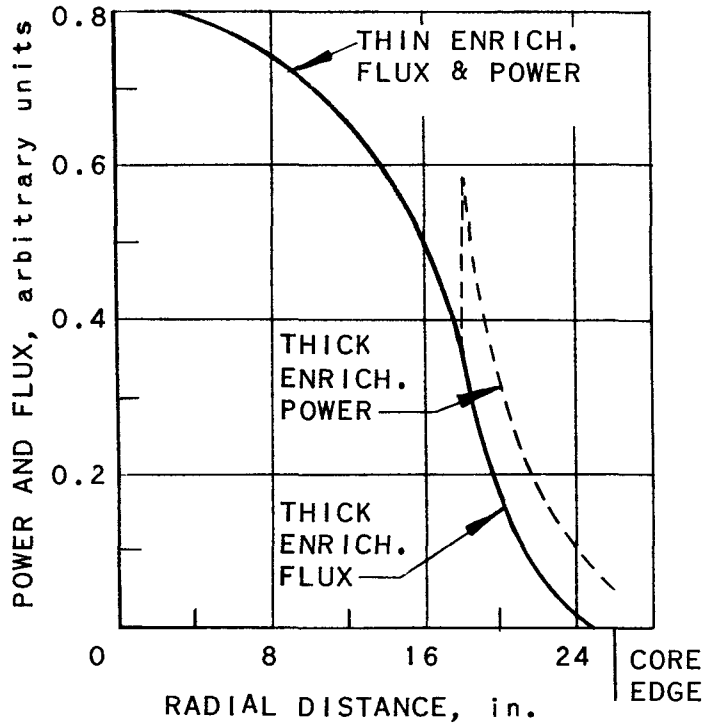

FIG. 10
RADIAL FLUX AND POWER DISTRIBUTION IN ENRICHED ELEMENTS OF LOADING #46

15

Table IV

FLUX AND POWER DISTRIBUTIONS AT ROOM TEMPERATURE IN LOADING #46

Axial Maximum to Average Power Density with Control Rods in Upper 71% of Fuel	2.17
Axial Buckling from the Flux	0.002025 cm^2 ± 20%
Reflector Savings of Control Rod Zone	27.6 ± 8 cm
Radial Maximum to Average Power Density (Ignoring Hot Spot Factors)	1.663
Radial Power Distributions:	
Thin Naturals	1.6%
Thin Enriched	64.6%
Thick Naturals	1.1%
Thick Enriched	32.7%

Using the relation:

$$\rho = 1 - \exp\left(-\sum_i \rho_i\right)$$

for obtaining large reactivities, it is found from Fig. 11 that the control rods are holding down 7.13% at cold clean criticality. Extrapolation yields an additional 6.82% in shutdown strength. A more accurate measure of the shutdown strength is had by determining B_m^2 of the upper rodded region from the axial flux plot, Fig. 9, as if it were an exponential assembly.[3] This yields a shutdown strength of 5.27%.

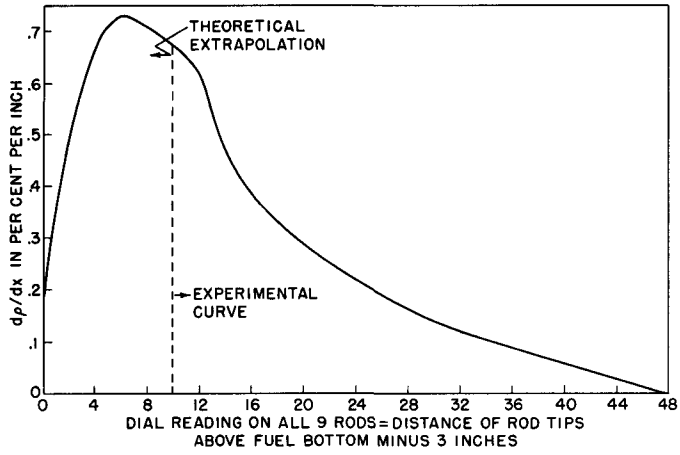

FIG. 11

DIFFERENTIAL WORTH OF ALL 9 CONTROL RODS AS A BANK AT ROOM TEMPERATURE IN LOADING #46.

[3] R. T. Bayard, "Control Rod Worth Studies on Seed and Blanket Reactors," Los Angeles Reactor Control Meeting, March 6, 1957.

F. Temperature Coefficient Measurements

The start-up heat exchanger, which utilizes auxiliary steam, was used to heat the reactor water to 325F (reactor pressure = 100 psig). Higher pressures were obtained by nuclear heat. Figure 12 shows the integrated temperature coefficient obtained from frequent critical measurements and control rod calibrations performed during the heating process. A preliminary comparison with the void coefficient shows that the effect of water density probably dominates the contributions to temperature coefficient.

Figure 13 shows the effect of temperature on differential rod worth, using the factor:

$$1 + \delta = \frac{\text{Differential rod worth at some temperature}}{\text{Room temperature differential rod worth at the same rod setting}} .$$

It is estimated that experimental errors lead to a 20% uncertainty in δ.

Since the temperature coefficient is a function of rod position and the rod worth is a function of temperature, there is no unique value for the integrated temperature coefficient. For example, three acceptable definitions are:

$$\int_{X(68)}^{X(489)} \left(\frac{d\rho}{dX}\right)_{T=68} dX = 2.47\% \quad ; \qquad (1)$$

$$\int_{X(68)}^{X(489)} \left(\frac{d\rho}{dX}\right)_{T=68} [1 + \delta(T)]\, dX = 2.93\% \text{ (from Fig. 12)} \; ; \qquad (2)$$

$$[1 + \delta(489)] \int_{X(68)}^{X(489)} \left(\frac{d\rho}{dX}\right)_{T=68} dX = 1.3 \times 2.47\% = 3.21\% \quad , \qquad (3)$$

where X(68) and X(489) are the critical positions at room temperature and 600 psig, respectively.

These values, which pertain to a reactor whose control rod bank is in the 11 in. to 15-in. position, are, of course, appreciably larger than the corresponding value for the reactor with all rods out. (The latter, from Table VI, is 7.13% - 6.46% = 0.67%, but is very inaccurate due to uncertainties in the value of δ.)

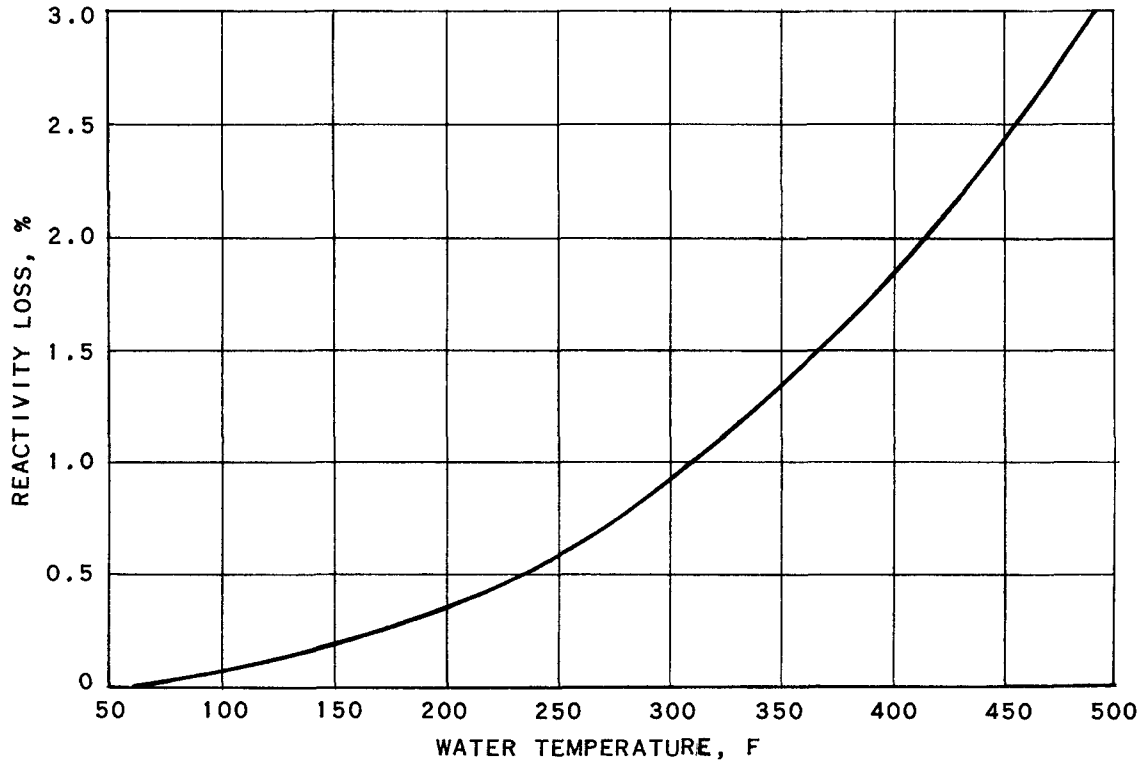

FIG. 12
INTEGRATED TEMPERATURE COEFFICIENT
FOR LOADING #46 (UNPOISONED)

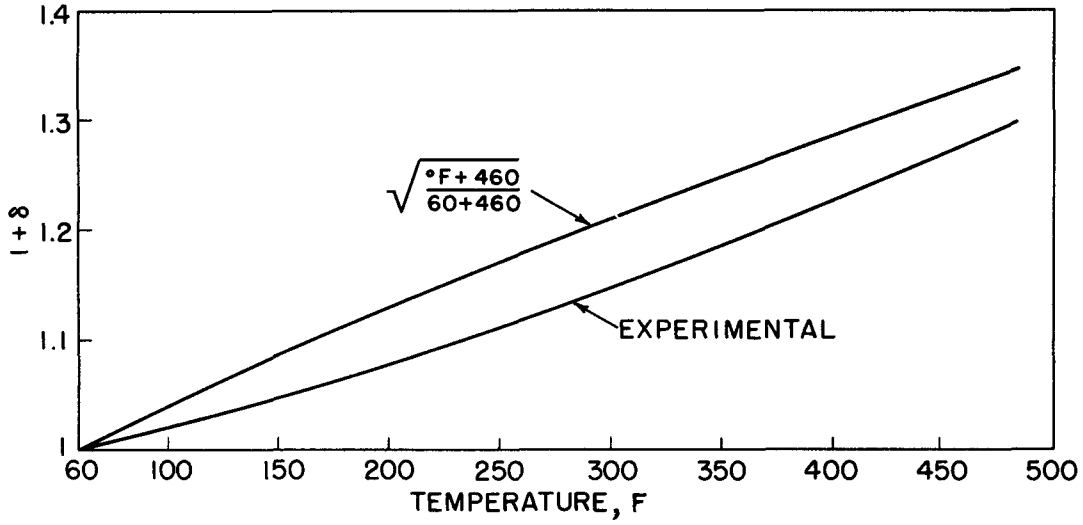

FIG. 13
EFFECT OF TEMPERATURE ON
DIFFERENTIAL ROD WORTH

III. POWER GENERATION EXPERIMENTS

The purpose of this program was to make a quick survey of the power capabilities and performance of the reactor. No attempt was made to study and measure in detail the power performance at one particular condition. Hence, some of the numerical information presented should be regarded as being of a preliminary nature. The phases in this program were:

(1) low-pressure power operation,
(2) 600-psig operation without, then with, the turbine, and
(3) steady operation, building up equilibrium xenon.

A. Low-Pressure Power Operation

The normal procedure in coming to 600 psi involves heating the reactor water to 100 psi with building steam via a heat exchanger, and then using reactor heat, holding the amount of boiling to insignificance. During initial experiments, however, water heating was accomplished at all pressures with nuclear heat.

During the course of the experiment (see Table V) the reactor was essentially free of xenon and contained no boric acid. The reactivity was compensated by steam voids, probably below 0.4%. The control rods were level as a bank in the $11\frac{1}{2}$- to $12\frac{1}{2}$-in. region, gradually coming out as the temperature rose. What may have been the first boiling occurred at atmospheric pressure and, initially at least, when some regions of the water in the vessel may not have been at 212F.

It is evident from this experiment that some of the variables possibly affecting the oscillatory tendency are: pressure, power level, feed-water flow, and water level relative to the top of the shroud. The shroud is essentially a 2.8-ft chimney above the fuel. Natural convection within the vessel is rather restricted unless the water level is above the shroud.

Figure 14 shows the character of the oscillation referred to in Table V. For the largest oscillations the reactivity amplitude is only ± 0.067% - well under the probable maximum reactivity that could have been in voids (0.4%). Whether this behavior is of a type hitherto unobserved in boiling reactors is open to some speculation. It is different in a number of respects from the chugging phenomena that have been reported:[4,5,6]

[4] J. R. Dietrich and D. C. Layman, "Transient and Steady-State Characteristics of a Boiling Reactor," ANL-5211 (February, 1954)

[5] S. G. Forbes, F. Schroeder and W. E. Nyer, "Instability in SPERT-I," Nucleonics, Vol. 15, No. 1, p 41 (1957)

[6] J. A. Thie, "An Experimental and Theoretical Investigation of Boiling Reactor Instabilities," Pittsburgh A. N. S. Meeting, June, 1957

Table V

PROGRESSION OF EVENTS IN THE FIRST EBWR NUCLEAR HEATING EXPERIMENT, DECEMBER 18, 1956

Time	Pressure, psig	Water Line Temperature, F	Feedwater Flow, gpm	Power Oscillations: Dominant Frequency, cps	Power Oscillations: 200 x Amplitude Mean Power	Approximate Power, kw	Remarks
12:00 A.M.	0	66	0	-	0	1800	Temperature starts to rise at rate of 0.2F/min from this initial value. This rate then increases appreciably, although power is constant, indicating failure of water line thermocouple to read a true average water temperature.
12:42	0	82	0	0.133	4	1800	A sharp increase in the temperature rise rate to 2F/min at the onset of oscillation is interpreted as an increase in the natural convection in the water line from the reactor.
12:51	0	100	0	0.151	6	1800	
12:59	0	129	0	0.178	9	1800	
1:00	0	131	0	0.125	5	1100	A power reduction affects the oscillation.
1:16	0	220	0	0.14	6	1100	
1:17	0	220	0	-	0	550	Oscillations have a threshold power of ~900 kw.
1:25	0	220	12	-	0	550	
1:33	0	245	12	0.167	18	1200	Greatest oscillatory tendency is found here.
1:59	0	250	12	0.167	18	1000	
2:00	0	250	0	0.050	10	1000	A third harmonic is quite noticeable.
2:04	0	250	0	0.050	10	100	
2:05	0	250	12	0.178	5	900	Water level is believed to be crossing the top of the shroud (which is about 3 ft above the fuel) approximately now.
2:14	0	250	12	0.178	5	900	
2:15	0	250	0	-	0	900	Oscillatory tendency is reduced in the absence of feedwater.
2:40	10	256	0	0.266	9	1800	In coming up in power an oscillation threshold at ~1000 kw was observed.
3:25	80	305	0	0.30	4	2700	
3:35	110	310	0	0.0934	6	2700	Oscillatory character is insensitive to feed-water flow here.
3:50	130	345	0	-	0	2700	No oscillations occur at pressures beyond 130 psig at this power level.

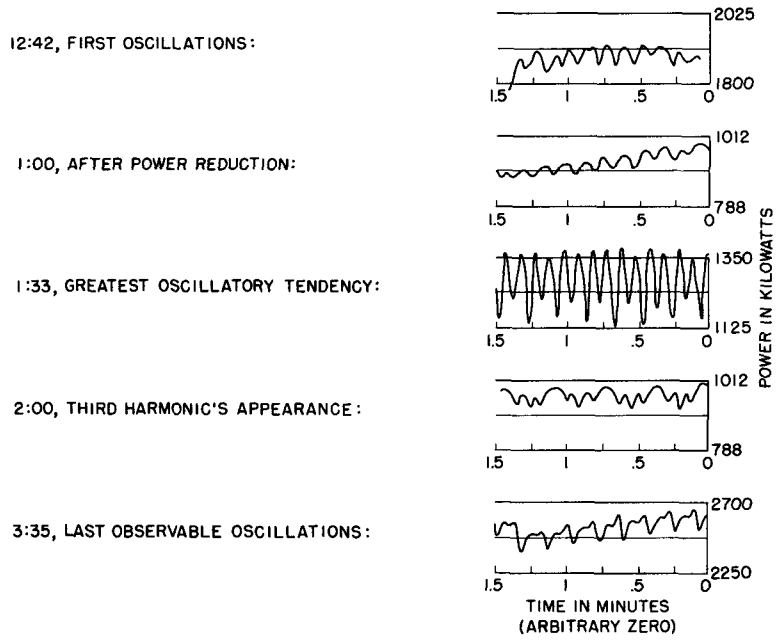

FIG. 14
POWER OSCILLATIONS AT LOW PRESSURE

(1) The harmonic content is high, in view of small amplitudes involved.
(2) The fundamental frequency, as well as harmonic structure, is sensitive to quantities affecting flow conditions.
(3) The power density and reactivity available for voids are quite low.

Figure 15 shows critical control rod positions obtained at various temperatures and essentially zero power.

B. Boric Acid in the Pressurized Reactor

Initial operation at 20 mw was with borated water, since this reduced the reactivity in voids and also reduced the power density by enabling the control rods to be further out. Borating also had the advantage, especially in combination with xenon buildup, of providing calibration points over extended regions of rod travel.

Four methods are available for the determination of the concentration:

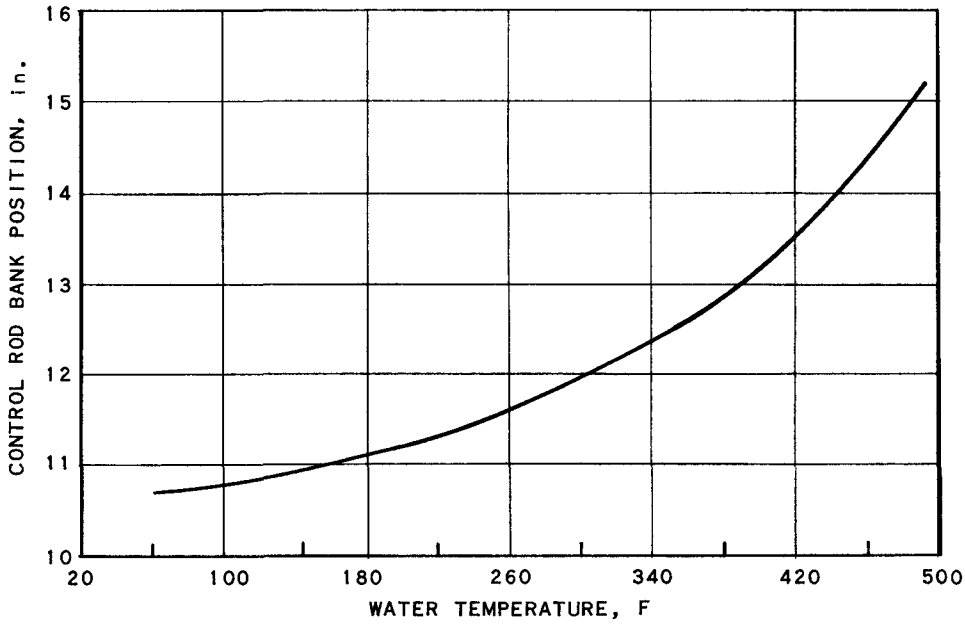

FIG. 15
POSITION OF CONTROL ROD BANK VS TEMPERATURE
FOR LOADING #46 (UNPOISONED)

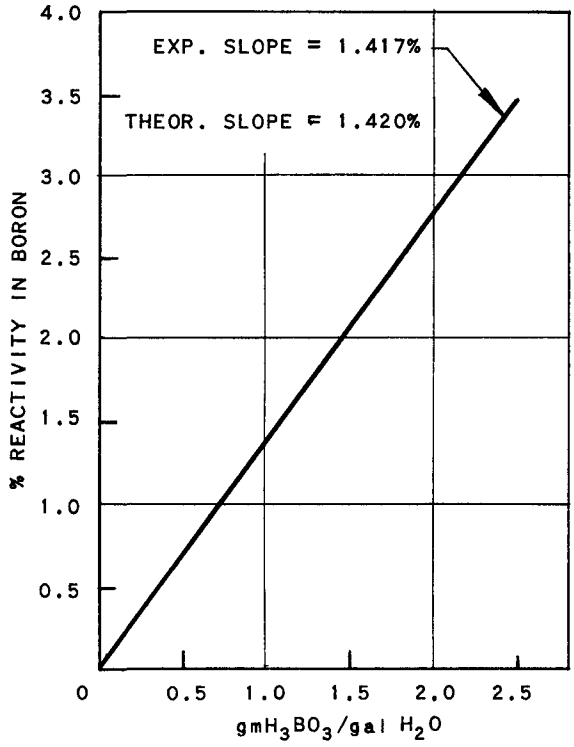

FIG. 16
REACTIVITY IN BORIC ACID
ADDITION TO LOADING #46

(1) the quotient of the amount added and the reactor water volume;
(2) titration of a sample of the reactor water;
(3) comparison of neutron absorption of the reactor water sample with that of a standard boric acid solution;[7]
(4) the quotient of the measured reactivity change and the value 1.660%/gram of H_3BO_3/gal. (calculated from reactor theory at 600 psi and 0% voids).

Methods (2) and (3) agreed within 4%. The average of (1), (2) and (3) in grams per gallon multiplied by 1.660 is seen in Fig. 16 to agree well with the reactivity from the calibration of control rods as implied by (4).

Removal of the boric acid was accomplished while the reactor ran at 20 mw with equilibrium xenon by circulating the water continuously at 9.25 gpm through an ion exchange column. It is easily shown that the removal law is

$$\frac{dM}{dV} = \left(\frac{dM}{dV}\right)_{t=0} \exp\left(-\frac{FE}{V}\, t\right) \quad ,$$

where M is the boric acid mass in volume V; F is the flow rate; and E is the column efficiency. The theory is borne out in Fig. 17, which shows E to be 0.8 to 1.

Various amounts of boric acid and xenon placed the rod bank in the various positions required for calibration by long periods. The technique finally found adequate for accurate calibration in the presence of transient xenon, temperature changes, and boric acid concentration changes was the following: five periods were done in succession with all but the third at the same rod position. Plotting the similar periods or reactivities against time gives the proper value for use with the third period.

C. High-Power Operation

When the control rods are pulled out from their critical position at 600 psig, the reactivity addition is compensated by steam voids, manual or automatic pressure regulation preventing the pressure from rising further. The definition of this reactivity in voids used below is that corresponding to the positive period which would result from the collapse of all voids. (An alternate and numerically different definition would be the negative period resulting from the appearance of voids with control rods in the zero-power critical position.)

---

[7] R. A. Mattson, "The Determination of Soluble Poison Concentrations in H_2O," Master's Thesis, Michigan College of Mining and Technology (1957)

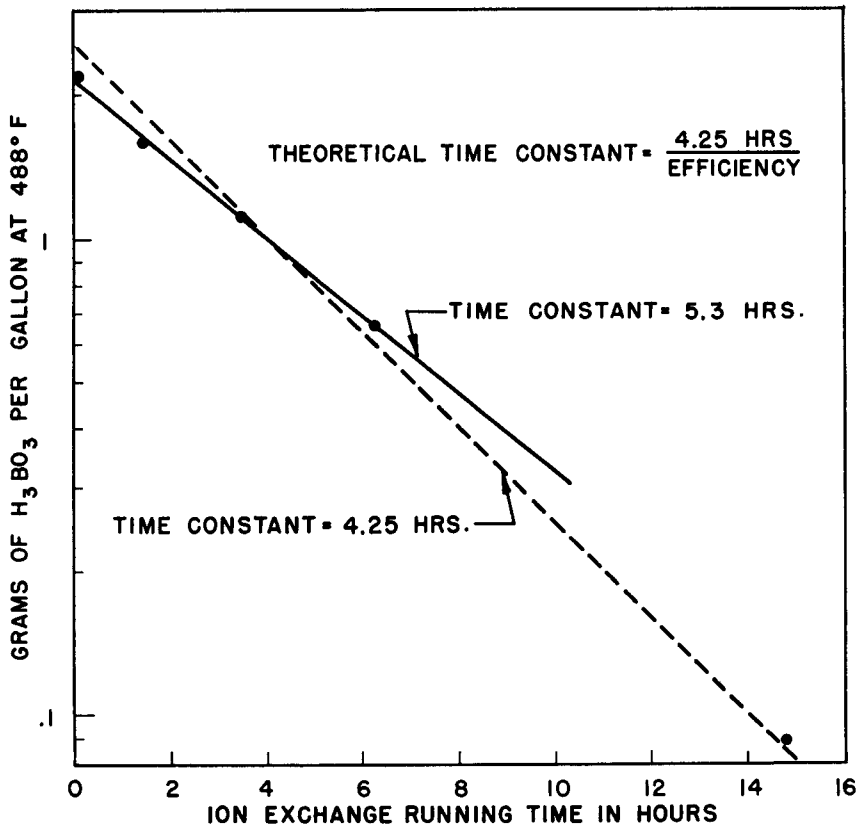

FIG. 17
BORIC ACID REMOVAL FROM EBWR
DURING 20-mw OPERATION

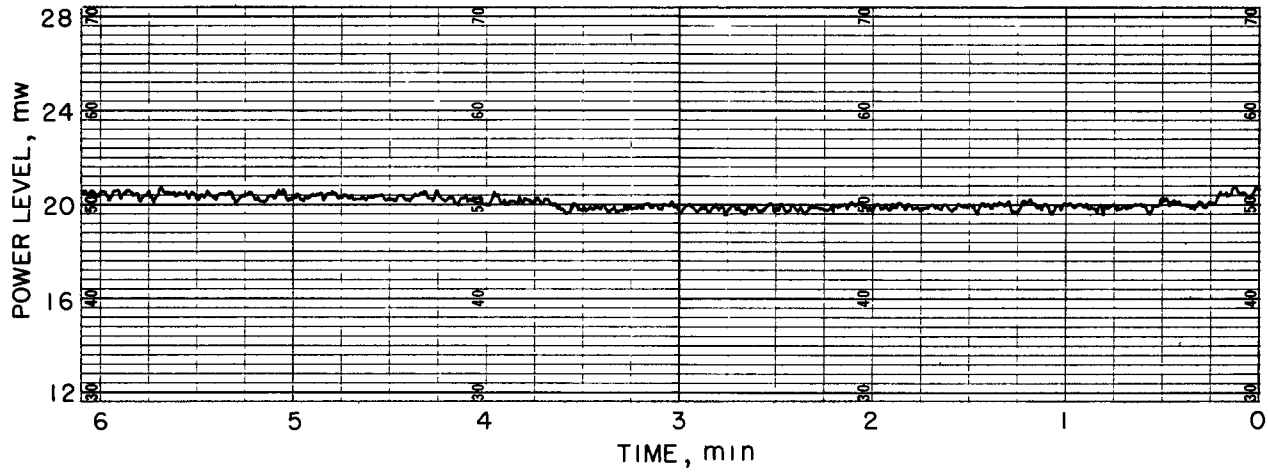

FIG 18
ION CHAMBER RECORD AT 20-mw OPERATION

= 4

Figure 18 shows a typical ion chamber record when the reactor is at equilibrium. Any oscillatory tendency present in the 600-psig, 20-mw condition is obviously less than the boiling noise. Mild disturbances (by control rods, feed water, or pressure) of the reactor in this condition fail to excite oscillations of the type found either at low pressures or in other reactors.

Figures 19, 20 and 21 show the dependence of the reactivity in voids on control rod positions and boration. All powers are measured from feed water and steam flows. Qualitatively, the behavior is as expected. The reactivity is obtained from the rod positions at power and at zero-power criticality, using a calibration based on periods at 600 psig and zero voids. Because of the numerous corrections applied to the data before plotting, it is believed that the absolute accuracy of the ordinate of these figures is ± 25%.

From the value of 0.724% reactivity in voids at 19.62 mw and 2.373 gm of H_3BO_3/gal, and the theoretical void coefficient at 7.5% voids, $\frac{d\rho}{dV} = -0.1163$, from Table VII it is possible to compute the average void:

$$\overline{V} = \frac{-0.00724}{-0.1163 + \left(\frac{\overline{V}}{2} = 0.075\right)\frac{d^2\rho}{dV^2}}$$

Using

$$d^2\rho/dV^2 \cong -0.293 \quad ,$$

one obtains:

$$\overline{V} = 6.93\% \quad .$$

Heat transfer calculations[8] (corrected slightly for the presence of thin enriched elements in the center of the reactor) give 7.7 ± 1.1%, and the agreement is as well as can be expected. In all cases the void percentages refer to coolant channel water only, and the volume averaged voids differ little from the statistically weighted average.

The slope of the line in Fig. 20 is considerably steeper than would be expected from the void percentages just given. An unexplained reactivity shift of several tenths of a per cent during the experiment might account for the anomaly.

---

[8] R. J. Weatherhead, private communication.

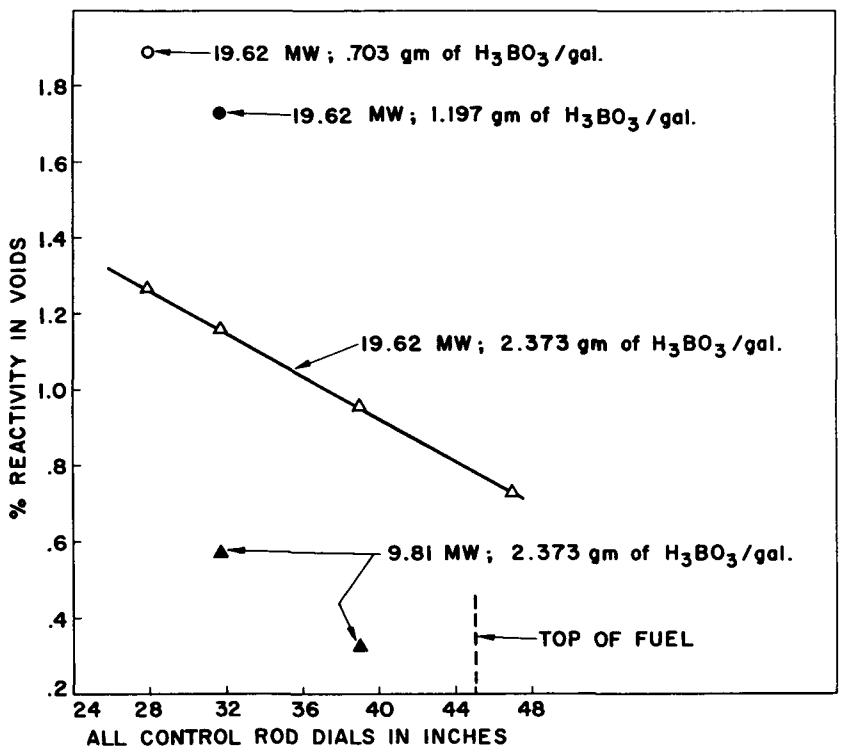

FIG. 19
REACTIVITY IN VOIDS AT 620 psig

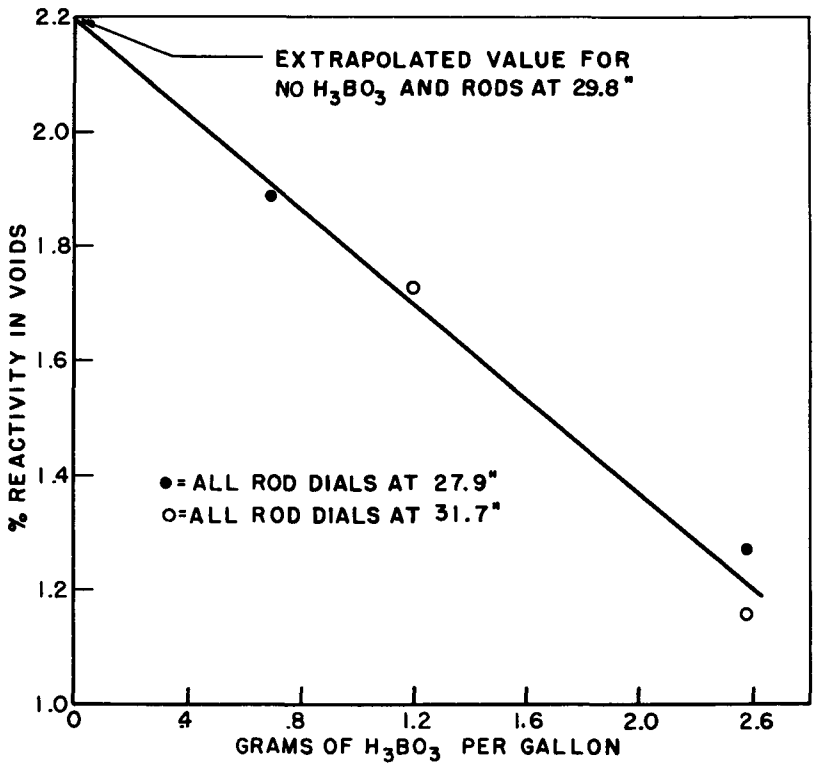

FIG. 20
EFFECT OF H_3BO_3 ON REACTIVITY IN VOIDS

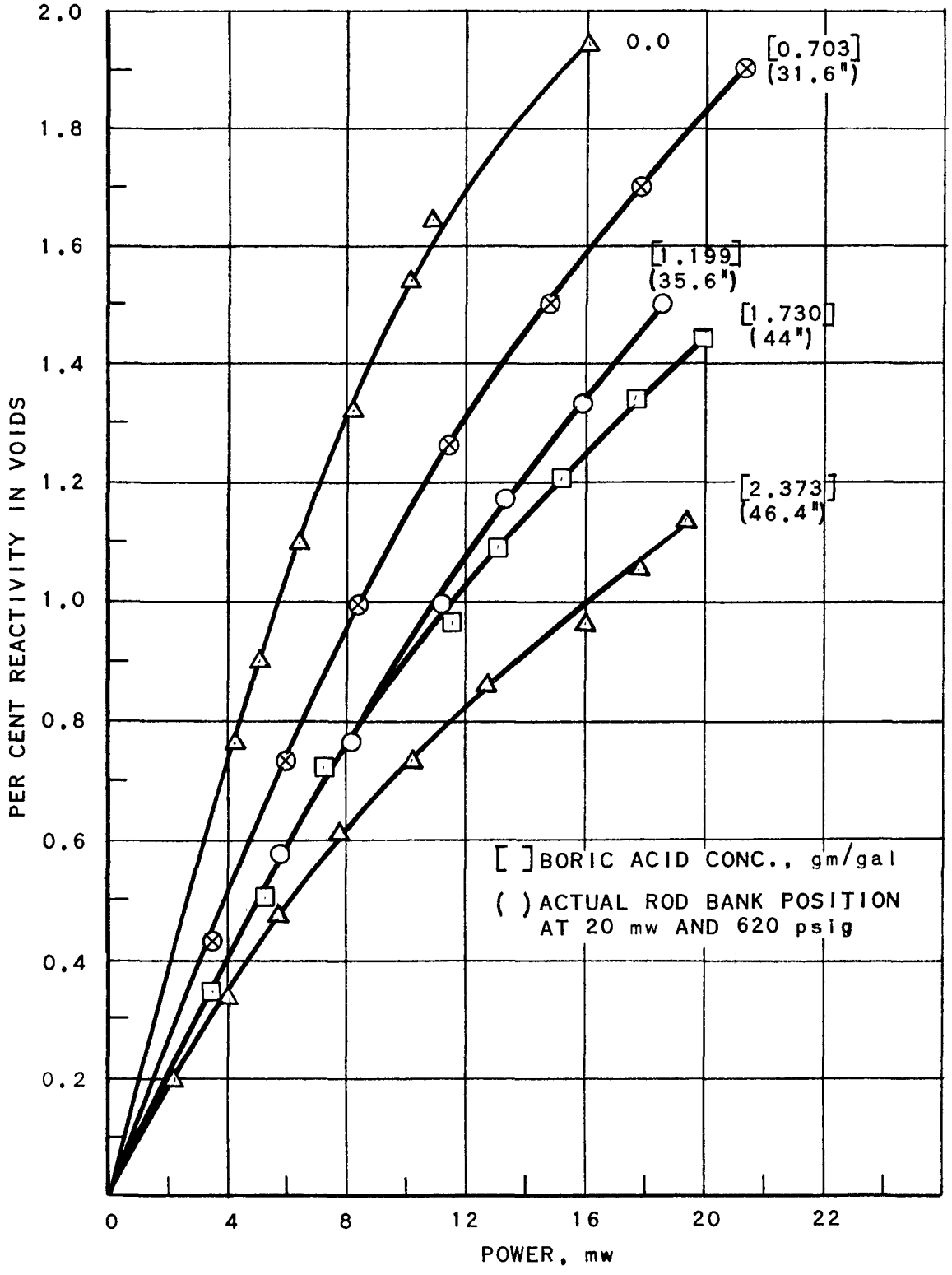

FIG. 21
REACTIVITY IN VOIDS AS INFLUENCED BY POWER, ROD POSITION AND BORIC ACID

The reactivity status of loading #46, as determined from the above experiments, is as follows:

Table VI

REACTIVITIES OF LOADING #46

Integral of 64F differential rod worth curve from unpoisoned criticality at 64F to all out: 7.40% Reactivity	7.13%
Integral of 483F differential rod worth curve from unpoisoned zero power criticality at 483F to all out: 6.57% Reactivity	6.46%
Reactivity in xenon (theoretical value)	2.20%
Reactivity in samarium (theoretical value)	0.75%
Residual reactivity at 483F and all rods out for burnup and voids	3.51%

Use is made of the relation:

$$\rho = 1 - \exp\left(- \sum_i \rho_i\right)$$

in obtaining the large positive reactivities in Table VI. The residual reactivity of 3.51% compares quite favorably with the theoretical value of 3.40% in Table VII (see the Appendix).

APPENDIX

THEORETICAL BASIS OF REACTOR AND CONTROL ROD REACTIVITIES

B. Maxon* and J. A. Thie

As pointed out in Section IIA, 2-group theory overestimates the reactivity by 3.39% and overestimates the void coefficient by about 0.067. This theory has been adequately presented,[9,10] and only modifications of it will be discussed here. The modified theory differs from previously used methods in that: (1) fast leakage is described by exp (τB^2) (rather than $1 + \tau B^2$); and (2) the U^{238} resonance integral is taken to be 1.209 times larger than that based on

$$7.5\left(1 + \frac{3.4}{0.1 + \frac{M}{S}}\right) \text{barns}$$

previously used.

These modifications can be rationalized both empirically and theoretically: The reactivity error between theory and experiment vanishes, while the void coefficient discrepancy virtually vanishes. The theoretical basis for adjusting the resonance integral is threefold:

(1) Its uncertainty is larger than any other major parameter of 2-group theory.
(2) Macklin and Pomerance[11] quote a value somewhat larger than 7.5 barns.
(3) Excessive non-fission capture of U^{235}, if not taken into account elsewhere, acts to increase the resonance integral.

Lattice constants and reactivities as computed by the modified theory are listed in Table VII. The approximation to loading #19 is slightly supercritical by the reactivity difference between the approximation and the actual loading. Perturbation theory results for loading #33 and #46 are obtained by applying 2-group perturbation theory to thin enriched loadings.

---

*Loaned Employee from American Machine and Foundry

[9] ANL-5607, "The EBWR" (May, 1957)

[10] Reactor Engineering Division Quarterly, ANL-5561 (December, 1955) p. 18

[11] R. L. Macklin, H. S. Pomerance, "Resonance Capture Integrals." Proceedings of the International Conference on the Peaceful Uses of Atomic Energy held in Geneva, 8 August-20 August, 1955, Vol. 5, p. 96.

Table VII

CALCULATED LATTICE CONSTANTS

Loading	19[a]	ET[b]	ET[b]	ET[b]	33	33	33	ET[b]	ET[b]	46	46	46	46
% ρ in Xe + Sm	0	0	0	0	0	0	0	2.95	2.95	2.95	2.95	2.01	2.01
gm of H_3BO_3/gal	0	2.235	2.235	2.235	2.235	2.235	2.235	0	0	0	0	2.373	2.373
Temperature, F	68	68	68	68	68	68	68	486	486	486	486	486	486
% Plate Voids	0	0	0	0	0	0	0	0	15	0	15	0	15
No. of Elements	81	112	112	112	112	112	112	114	114	114	114	114	114
ϵ	1.0367	1.0266	1.0282	1.0303				1.0300	1.0324				
ηU^{235}	2.053	2.053	2.053	2.053				2.053	2.053				
p	0.8425	0.8665	0.8553	0.8358				0.8371	0.8151				
$\left(\frac{U^{235}\text{ Absorption}}{\text{Total Absorption}}\right)$	0.6052	0.6126	0.6252	0.6428				0.6400	0.6521				
k_∞	1.0852	1.1187	1.1287	1.1363				1.1328	1.1264				
L^2, cm^2	3.017	2.838	3.130	3.527				6.310	7.270				
τ, cm^2	34.75	34.46	39.76	49.17				47.59	58.42				
Refl. Savings, cm	7.02	7.02	7.54	8.25				9.50	10.62				
$\Sigma_{as}^{(c)}$, cm^{-1}	0.09611	0.09795	0.09681	0.09527				0.09786	0.09671				
Σ_{af}, cm^{-1}	0.03196	0.03229	0.02985	0.02653				0.02702	0.02409				
B^2, cm^{-2}	0.002047	0.001665	0.001640	0.001608				0.001538	0.001492				
ρ	0.0043	0.0488	0.0494	0.0421	0.0130	0.0121	0.0039	0.0410	0.0208	0.0340	0.0113	0.01[d]	-0.0075[d]
$(d\rho/dV)$		0.0064	-0.0536		-0.0085	-0.0604		-0.1342		-0.1513		-0.1163	

(a) Actually: 13.01 T + 13.01 H + 27.49 ET + 27.49 EH
(b) All elements are thin enriched
(c) Equivalent 2200 m/sec value
(d) Includes a 0.6% reactivity gain observed experimentally

The integral rod worth for loading #46 at room temperature is plotted in Fig. 22. To determine the worth of the rods at higher temperatures, the factor

$$(1+\delta)_T = \frac{\text{Differential Rod Worth at Temperature T}}{\text{Differential Rod Worth at Room Temperature at Same Position}}$$

was defined. This factor is useful if it can be considered independent of rod position, since it is not necessary to measure the differential worth over the entire range of rod travel. Theoretical methods, as well as experimental methods, were used to check the validity of the constancy of $(1+\delta)_T$ with rod position. It can be shown that the differential rod worth at any position may be expressed as:

$$\frac{\delta\rho}{\delta X} = \frac{2}{\pi} M_T^2 B_Z^2 \exp\left[-M_T^2 (B_{1Z}^2 - B_{OZ}^2)\right] \qquad (1)$$

where

B_{OZ}^2 = Axial Buckling with Rods Out

B_{1Z}^2 = Axial Buckling with Rods in, at X

$= (\pi/S_T + X + S_Z')^2$

X = Distance from Bottom of Fuel to Rod Bank

M_T^2 = Migration Area at Temperature T

S_Z' = Effective Savings of Rodded Region on Non-Rodded Core Region

S_T = Reflector Savings at Reactor Bottom

Equation (1) and the experimental rod worth at 68F (Fig. 22) were used to determine the curve plotted in Fig. 23. From this curve and the values of M_T^2 and S_T at some temperature other than 68F, the dependence of $(1+\delta)_T$ with rod position may be obtained. It was found at 488F that $(1+\delta)_{488}$ was indeed independent of position. Experimentally, $(1+\delta)_T$ was also found to be approximately position independent. At 488F $(1+\delta)_T$ was found theoretically to be 1.334 ± 0.05 as compared to the experimental value of 1.306 ± 0.06.

This method may be employed to estimate the rod worth at any power level provided the average voids in the non-rodded section as a function of rodposition are known. Quantitatively, the method has experimental support for integral rod worths obtained during xenon buildup.

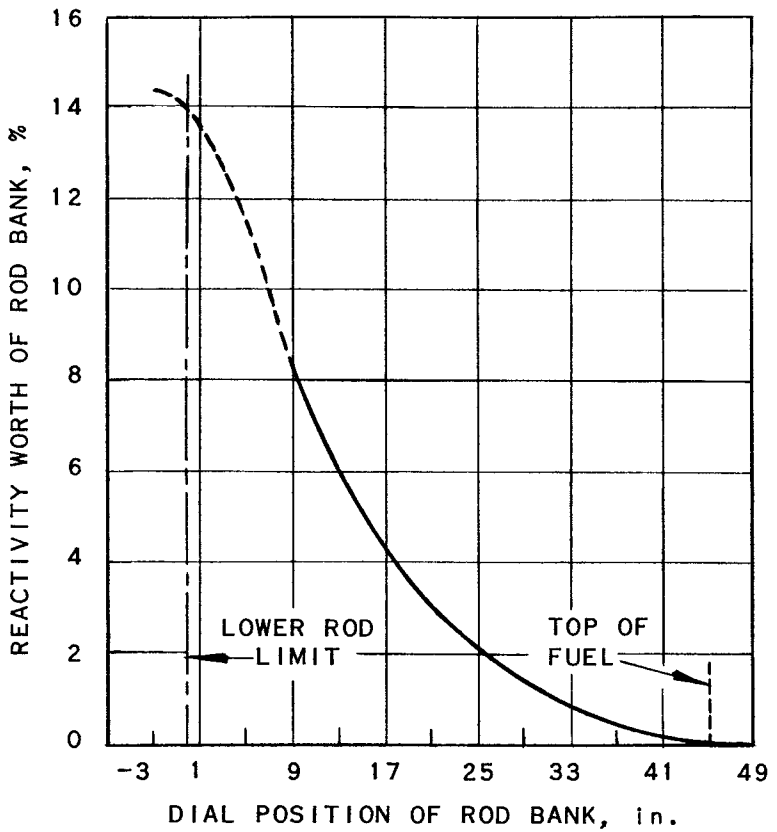

FIG. 22
INTEGRAL ROD WORTH FOR
LOADING #46 AT 68 F

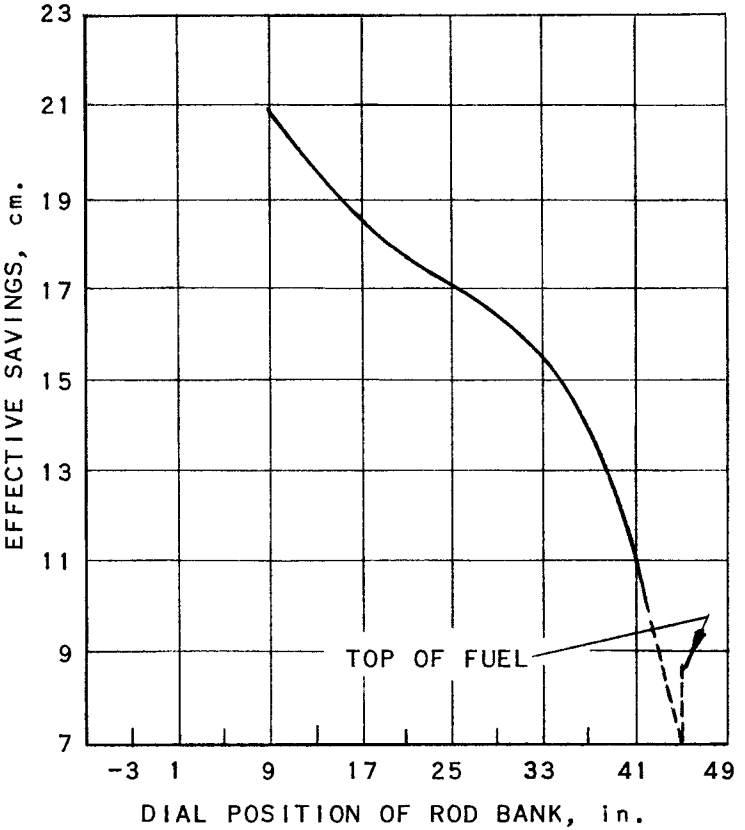

FIG. 23
EFFECTIVE SAVINGS OF RODDED
REGION AS A FUNCTION
OF ROD BANK POSITION